Earth Surf. Dynam. Discuss., 2, 773–822, 2014
www.earth-surf-dynam-discuss.net/2/773/2014/
doi:10.5194/esurfd-2-773-2014

Earth Surface Dynamics Discussions
Open Access

Recalculation of bedload transport observations in Swiss mountain rivers using the model sedFlow

F. U. M. Heimann[1,2], D. Rickenmann[1], M. Böckli[1], A. Badoux[1], J. M. Turowski[3,1], and J. W. Kirchner[2,1]

[1]WSL Swiss Federal Institute for Forest, Snow and Landscape Research, 8903 Birmensdorf, Switzerland
[2]Department of Environmental System Sciences, ETH Zurich, 8092 Zurich, Switzerland
[3]Helmholtz Centre Potsdam, GFZ German Research Centre for Geosciences, Telegrafenberg, 14473 Potsdam, Germany

Received: 20 June 2014 – Accepted: 3 July 2014 – Published: 24 July 2014

Correspondence to: F. U. M. Heimann (florian.heimann@wsl.ch)

Published by Copernicus Publications on behalf of the European Geosciences Union.

Abstract

Only few validated numeric models are available for the simulation of bedload transport dynamics in mountain streams. In this study, the recently developed modelling tool sedFlow has been applied to simulate bedload transport in two Swiss mountain streams. It is shown that sedFlow can be used to successfully reproduce observations from historic bedload transport events with reasonable parameter set-ups. The simulation results shed light on the difficulties that arise with traditional flow resistance estimation methods when macro-roughness is present. In addition, our results demonstrate that greatly simplified hydraulic routing schemes, such as kinematic wave or uniform discharge approaches, are probably sufficient for a good representation of bedload transport processes in steep mountain streams. The influence of different parameters is qualitatively evaluated in a simple sensitivity study. This proof-of-concept study demonstrates the usefulness of sedFlow for a range of practical applications in alpine mountain streams.

1 Introduction

The rolling, sliding or saltating transport of sediment grains along river beds, which is summarised as bedload transport, represents one of the main morphodynamic processes in mountain streams. However, bedload transport has implications which go beyond mere morphodynamics. It has a considerable ecologic influence by reorganising the bed and thus potential spawning grounds. Because bedload transport can amplify the impact of severe flood events, it is also important in natural hazard management. This wide range of implications is reflected in numerous applied engineering projects, which evaluate potential bedload transport using different one- or two-dimensional simulation models. A summary of the applied aspects of bedload transport assessment has been given by Habersack et al. (2011).

The available models for the simulation of sediment transport may be subdivided into two groups. The first group of models does not focus on process details. It rather sees fluvial sediment transport as a part of a network of interacting processes within the landscape. Therefore, such models use simplified representations of river hydraulics and are often combined with hydrologic or soil erosion model components. Large-scale spatial resolutions and fast calculations are common in this group of models. The models SHETRAN (Lukey et al., 2000; Bathurst et al., 2010), DHSVM (Doten et al., 2006) and others (e.g., Mouri et al., 2011) fall in this group. The model SHESED (Wicks and Bathurst, 1996) also combines sediment transport routines with hydrologic and soil erosion routines, but without the strong simplifications (and associated efficiency gains) of the models mentioned above.

The second group of models concentrates on hydraulic processes as the main driving factor of sediment transport. Therefore, such models commonly solve the full Saint Venant equations, but neglect any processes outside the channel. Small-scale spatial resolutions and slow calculations are common in this group of models. The models 3ST1D (Papanicolaou et al., 2004), HEC6 (Bhowmik et al., 2008), SEDROUT (Ferguson et al., 2001), GSTARS (Hall and Cratchley, 2006), 2D Flumen (Beffa, 2005), Basement (Faeh et al., 2011) and others (e.g., Lopez and Falcon, 1999; García-Martinez et al., 2006; Li et al., 2008) fall in this group.

Similar to Tom$^{\mathrm{Sed}}$ (formerly known as SETRAC) (Chiari et al., 2010), the model sedFlow (this article) is intended to bridge the gap between these two groups of models by providing good representation of fluvial bedload transport processes at intermediate spatial scales and high calculation speeds. Here, the focus is not on the details of the temporal evolution of sediment transport, but rather on a realistic reproduction of the overall morphodynamic results of sediment transport events such as major floods.

In spite of the considerable need for modelling tools in scientific and engineering applications and in spite of the interest in the relevant physical processes, relatively few scientific studies have worked on bedload transport in alpine streams. This is partly due to the complex measurement conditions in gravel-bed rivers (Bunte et al., 2008; Gray

ESURFD
2, 773–822, 2014

et al., 2010). Because of these difficulties, there are relatively few data sets available for deriving conceptual models or for validating and testing numeric models.

Based on the available field observations, it has become clear that river bed morphology and thus hydraulic processes become increasingly complex as channel gradients become steeper. The range of observed grain diameters becomes larger, which entails more complex grain-grain and grain-flow interactions as well. Rickenmann and Recking (2011) have shown that a considerable part of the river's shear stress is consumed by turbulence due to complex bed morphology summarised as macro-roughness. They also suggested an approach to quantitatively estimate the impact of macro-roughness based on the relative flow depth compared to a characteristic grain diameter. Lamb et al. (2008) and Bunte et al. (2013) have discussed that in steep channels higher energies are needed for the initiation of bedload motion as compared to channels with gentle slopes. Turowski et al. (2011) have shown that the conditions for the initiation of bedload motion vary in time and are a function of the conditions at the end of the last bedload transport event. Parker (2008) and Wilcock and Crowe (2003) have discussed and proposed approaches for a simple consideration of grain-grain interactions in so-called hiding functions. Finally, several methods have been suggested for the quantitative estimation of bedload transport in alpine streams. Some of these methods are based on flume experiments such as those of Rickenmann (2001) and Wilcock and Crowe (2003) and some are based on field observations such as the those of Recking (2010) and Recking (2013). For recent examples of application and discussion of the conceptual models and methods mentioned in this paragraph see Chiari and Rickenmann (2011), Nitsche et al. (2011) and Rickenmann (2012). A selection of such methods related to the estimation of bedload transport in steep channels has been implemented in the modelling tool sedFlow. The model architecture and implementation is described in detail in a companion article (Heimann et al., 2014), and is only briefly reviewed here. This program is intended for quantitatively simulating bedload transport processes in mountain streams. It has been developed to provide a tool which

ESURFD

2, 773–822, 2014

Recalculation of bedload transport observations

F. U. M. Heimann et al.

combines state of the art process representations with fast computational algorithms and user-friendly file formats for an easy pre- and post-processing of simulation data.

In this article, we show that sedFlow can reproduce observations from historical bedload transport events, using reasonable parameter set-ups. The results of this study may help to interpret simulation results produced with sedFlow in applied engineering projects. Experiences with the simulation tool are discussed with respect to the problems of traditional flow resistance estimation methods to consider the influence of large blocks. Further on, the uncertainty of very common graphical representations of bedload transport reconstructions is highlighted based on the results of a simple sensitivity study.

2 Material and methods

For our study we selected the two rivers, the Kleine Emme and Brenno in Switzerland (Figs. 1 and 2). The Kleine Emme was chosen because extensive data to validate and test the sedFlow model are available for this catchment. The river Brenno was selected as a complementary case study to cover a wider range of channel gradients and streambed morphology.

In this article we differentiate between net and gross channel gradients in the context of sills. Net channel gradients are defined as gross channel gradients minus the elevation differences attributable to sills or other drop-down structures.

2.1 General catchment characteristics

The Kleine Emme is a mountain river in central Switzerland (Fig. 1). It drains an area of 477 km^2 and flows into the Reuss at Reussegg. In the Kleine Emme, the net channel gradient averages 0.7 % and has a maximum of 3.7 %. Near Doppleschwand the in-situ bedrock is close to the surface, limiting the alluvium that can potentially be eroded. Further downstream the river was channelised in the late 19th and early 20th century. To

Discussion Paper | Discussion Paper | Discussion Paper | Discussion Paper |

ESURFD

2, 773–822, 2014

Recalculation of bedload transport observations

F. U. M. Heimann et al.

mitigate the subsequent erosion, the bed was stabilised in the early 20th centuries with numerous sills (documented by Geoportal Kanton Luzern, 2013). The Kleine Emme is an alpine mountain river catchment with gentle slopes, without glaciers or debris flow inputs and with only very moderate influence from hydro power installations, but with intensive modifications by fluvial engineering.

The Brenno is situated in southern Switzerland (Fig. 2) and drains into the river Ticino. Its drainage area is 397 km^2 and its channel gradient averages 2.7 %, with a maximum of 15 %. As there are no sills in the Brenno, the net and gross gradients are the same. About 1 % of the catchment is glaciated. Especially in the northern and eastern part of the catchment, its hydrology is substantially influenced by hydropower (Fig. 2). The water used for hydropower is returned to the river Ticino at Biasca. The tributaries Riale Riascio and Ri di Soi are currently the most important sediment sources to the Brenno river (Table 1). The sediment input from the Riale Riascio is dominated by debris flows, while the larger subcatchment Ri di Soi delivers sediment both as debris flows and as fluvial bedload transport. Downstream of the confluences with these tributaries, the bed of the Brenno is stabilised by large blocks and the main channel shows pronounced knickpoints at these positions. Other tributaries on the western side of the Brenno catchment were very active in the decades 1970–1990, but their sediment delivery to the Brenno is much reduced at the time of writing due to intense torrent control works and sediment retention basins. The course of the Brenno is partially channelised and partially near-natural. The Brenno represents a moderately steep mountain stream influenced by glaciation, hydro power and debris flow inputs.

Several channel cross-sections are periodically surveyed for both rivers. In the case of the Kleine Emme, they are measured by the Swiss Federal Office for the Environment (FOEN) and in the case of the Brenno by the authorities of canton Ticino. Cross-sectional profiles are recorded at 200 m intervals in the Kleine Emme and at about 150 m intervals in the Brenno. For the Kleine Emme we used measurements from September 2000 and November 2005. For the Brenno we used measurements from

ESURFD
2, 773–822, 2014

Recalculation of bedload transport observations

F. U. M. Heimann et al.

April 1999 and June/July 2009. We selected our study reaches to overlap with these surveyed cross-sections.

Doppleschwand, about 25 km upstream of the Kleine Emme mouth, represents the upper boundary of our simulation reach. A very large and long-lasting flood event occured in August 2005, with a return period of slightly more than 50 years for the peak discharge. During this event, widespread flooding occured in the lowermost 5 km along the river in the area of Littau. Therefore, the lower boundary of our one-dimensional model simulations is the confluence of the Kleine Emme and the Renggbach (Fig. 1). At the Brenno, our study-reach extends from Olivone at the upper end to Biasca at the confluence with the Ticino river (Fig. 2).

2.2 Hydrology

For the Kleine Emme, discharge has been measured at Werthenstein since 1985 and at Littau/Emmen since 1978 (Fig. 1). Peak discharge at Littau/Emmen during the August 2005 flood was 650 $m^3 s^{-1}$. To account for the reduced catchment area of the Kleine Emme upstream of the Renggbach at the simulation outlet, the discharge at Littau/Emmen is reduced by 5 %. The discharge of the Rümlig tributary is estimated by the difference between Werthenstein and the simulation outlet. The discharge of the Fontanne has been simulated using the rainfall–runoff model PREVAH (Viviroli et al., 2009). The discharge of the headwater is estimated by the difference between the measured discharge at Werthenstein and the simulated Fontanne discharge.

Discharge for the Brenno has been measured at Loderio ever since the establishment of the hydropower reservoirs in the catchment in 1962. Peak discharge of 515 $m^3 s^{-1}$ was recorded during the July 1987 flood, corresponding to a return period of about 150 years. For the simulations, the discharge at Loderio has been distributed among the subcatchments according to rainfall–runoff simulations using the PREVAH model. The discharge is assumed to be zero at dams and reduced by the intake capacity at water intakes. In this reduction, we considered the regulations on the minimum residual discharge in the stream channel downstream of the water intake. The values

ESURFD
2, 773–822, 2014

Recalculation of bedload transport observations

F. U. M. Heimann et al.

of this minimum residual discharge were defined based on ecological aspects and vary with intake location and time of the year.

2.3 Channel morphology and bedload observations

2.3.1 Rectangular channels

For further processing and the use in the sedFlow model, the cross-section profiles were transformed into the width of a simple rectangular substitute channel as follows. For this transformation a representative discharge was defined as the mean of the peak discharge of simulation period and the discharge at the initiation of bedload motion, as these two values define the range of discharges relevant for bedload transport. The variable power equation flow resistance relation (Eq. 5) was used to translate discharge into flow depth based on the same grain size distributions as used in the simulations (Figs. 6 and 7). Then, a rectangular channel was found which has the same cross-sectional flow area and hydraulic radius as the original cross-section profile at this flow depth. The channel of the Kleine Emme has been regulated in the past and its geometry is well defined by a trapezoidal profile with steep banks. In contrast, the Brenno study reach is in a natural condition over most parts, including both more incised reaches with a well-defined width and depositional reaches in flatter areas with riparian forest. The latter reaches are characterised by river banks with gentle slopes. In such channels, a slight change of the representative discharge may result in a substantial change of the width of the rectangular substitute channel. Therefore, in the depositional reaches of the Brenno, the uncertainty in representative discharge entails a considerable uncertainty in substitute channel widths, which contrasts the smaller uncertainty in substitute channel widths in the incised Brenno reaches and in the Kleine Emme reaches with its steep banks.

ESURFD
2, 773–822, 2014

2.3.2 Reference data

To validate the sedFlow model, a reference is needed, to which the simulation results can be compared. Therefore, the bedload transport, which actually took place in the calibration period and which was not observed by itself, needs to be reconstructed from available observations. To volumetrically quantify the reconstructed bedload transport, the change in average bed level between the two cross-section surveys is multiplied with the mean of the substitute channel width of both profile measurements and with the distance to the next profile. These bed volume changes give an integrated value of the minmum bed material transported over the observation period. However, to obtain a complete sediment budget, data on bank erosion, lateral sediment input from tributaries and the material that leaves the catchment at the outflow have to be considered. At the Kleine Emme, bank erosion volumes were estimated from the difference between the FOEN cross-sectional profiles in 2000 and 2005 and from field assessment of the erosion scars (Flussbau AG, 2009; Hunzinger and Krähenbühl, 2008), and the sediment outflow was quantified based on data of regular gravel extraction at the confluence of the Kleine Emme with the Reuss (Hunzinger and Krähenbühl, 2008; Hunziker, Zarn and Partner AG, 2009). For the Brenno the lateral inputs by debris flows or fluvial bedload transport were estimated based on data from a number of preceding studies (Flussbau AG, 2003, 2005; Stricker, 2010), as listed in Table 1. The spatial pattern of changes in sediment transport as well as the absolute value of sediment transport is largely influenced by the sediment input from the tributaries. Thus, the uncertainty in the estimates of tributary sediment inputs largely determines the overall uncertainty in sediment transport in the Brenno. The sediment outflow at the mouth of the Brenno and thus the volume of the throughput load of the complete system is unknown. Therefore, we used the result of the sedFlow simulations as a best guess for this parameter.

2.3.3 Accumulated bedload transport

All volumetric data related to the sediment budget is summarised in the accumulated bedload transport (ABT) diagrams. ABT represents the net bedload amount, which has been transported through a given stream section during the period of interest (Chiari et al., 2010). It is a temporal integral of the transport rates and it is a spatial integral of the volumetric changes including bed net erosion and deposition, lateral inputs and sediment outflow. In this article, all ABT values include an assumed value of the pore volume fraction of 30 %. The ABT can be derived from the morphodynamic relation, which has been described by Exner in its continuous form (e.g., Parker, 2008):

$$(1-\eta_{\text{pore}})\frac{\delta z}{\delta t}+\frac{\delta q_{\text{b}}}{\delta x}=q_{\text{b}_{\text{lat}}}; \tag{1}$$

Here, η_{pore} is the pore volume fraction, z is elevation of channel bed, t is time, q_{b} is sediment flux per unit flow width, x is distance in flow direction and $q_{\text{b}_{\text{lat}}}$ is lateral sediment influx per unit flow width. It represents a balance of input and output volumes and it can be rewritten in a discretised form i.e. for a finite reach and period of time:

$$V_{\text{in}}-V_{\text{out}}-V_{\text{EroDepo}}=0; \tag{2}$$

$$V_{\text{in}}=V_{\text{inUp}}+V_{\text{inLat}}; \tag{3}$$

$$V_{\text{out}}=V_{\text{cap}}; \tag{4}$$

Here, V_{in} designates the volume of sediment that enters a reach, subdivided into the volume V_{inUp} coming from upstream and the volume V_{inLat} introduced laterally, e.g., by tributaries or bank erosion. V_{EroDepo} is the volume eroded or deposited in the reach, with positive values indicating deposition. V_{out} is the volume that exits the reach, which in case of unlimited (or at least sufficient) supply of material (Eq. 4) equals the volume V_{cap} corresponding to the transport capacity within the reach, multiplied by the duration of the considered period of time. Eq. (2) means that the difference of inputs and

ESURFD
2, 773–822, 2014

outputs is counterbalanced by erosion or deposition (Fig. 3). For erosion, the local V_{in} will always be smaller than V_{cap} and result in downstream increasing ABT. In the same way, deposition will result in a decreasing ABT, while a roughly constant ABT reflects throughflow of sediment without net erosion or deposition.

Grain size distributions (GSDs) have been estimated for different reaches, based on transect pebble counts using the method of Fehr (1987). In some cases at the Brenno, coarser sediment portions were added to the recorded GSDs, because coarse blocks have been underrepresented in the transect counts and thus the original transect GSDs partially led to unrealistic model behaviour. The measured GSDs were assumed to be representative for entire reaches, which are separated from each other by features such as confluences or considerable changes in channel gradient. This spatial extrapolation entails some uncertainty. The current GSD measurements, which were obtained after the end of the calibration period, are used as proxy estimates for the initial GSDs at the beginning of the calibration period. This time shift introduces additional uncertainty.

The bedload transport system of the Kleine Emme can be subdivided into two regimes (Fig. 4). In the upper part from km 25 to ~ 15, the bed is stabilised by in-situ bedrock and numerous sills. Therefore, the system is dominated by throughflow of sediment without considerable trends or jumps in the along-channel evolution of the ABT. In the lower part from km ~ 15 to 5, the bedload transport system is mainly influenced by sediment inputs from bank erosion during the 2005 flood event, which increase the downstream ABT in a step-like way.

The Brenno bedload transport system is mainly influenced by local elements (Fig. 5). The Riale Riascio at km 20.8 introduced a considerable amount of sediment to the system, resulting in a step-like downstream increase in the ABT. Large amounts of the material delivered by the Ri di Soi at km 18.1 have been deposited at the confluence. These deposits decreased upstream channel gradients and thus transport capacity. The lack of material coming from upstream is overcompensated by the input of the Ri di Soi. However, the excess material has been deposited shortly after the confluence. All processes around the confluence with the Ri di Soi are reflected in a pronounced

ESURFD
2, 773–822, 2014

negative and small positive peak in the along-channel evolution of the ABT. The following stretch down to km 10 exhibits erosion and deposition corresponding to the interaction of GSD, channel gradient and width, but without any overall erosion or deposition trend. At km 10 sediment has been anthropogenically extracted from the streambed by excavation, which results in a step-like downstream decrease of ABT. As the excavation reduced the amount of transported material down to the transport capacity of the stream, sediment bypasses the following reaches. At km 4.5, the deposits at the confluence with the Lesgiüna decrease the upstream slope and thus cause a drop in transport capacity. In the stretch from km 4.5 to 3, an increased channel width keeps the ABT at low values.

2.4 The model sedFlow

The bedload transport modelling tool sedFlow has been designed especially for application to mountain rivers. For this, it exhibits the following main features: (i) it uses state of the art approaches for calculating bedload transport in steep channels accounting for macro-roughness, (ii) it calculates several grain diameter fractions individually, i.e., fractional transport, (iii) it uses fast algorithms and thus can be used for modelling complete catchments and for scenario studies with automated calculation of many variations in the input data or parameter set-up. In the following we give a short overview over the essential components of sedFlow. For a detailed account of the model structure and implementation see Heimann et al. (2014). The current version of the sedFlow code and model can be downloaded at the following web page: www.wsl.ch/sedFlow.

Flow resistance is either calculated with the variable power equation of Ferguson (2007) according to Eq. (5) or with a grain-size-dependent Manning–Strickler

ESURFD
2, 773–822, 2014

equation (Eq. 6):

$$\frac{v_m}{v^*} = \frac{a_1 a_2 \left(\frac{r_\mathrm{h}}{D_{84}}\right)}{\sqrt{a_1^2 + a_2^2 \left(\frac{r_\mathrm{h}}{D_{84}}\right)^{\frac{5}{3}}}}; \tag{5}$$

$$\frac{v_m}{v^*} = a_1 \left(\frac{r_\mathrm{h}}{D_{84}}\right)^{\frac{1}{6}}; \tag{6}$$

Here, v_m is the average flow velocity, $v^* = \sqrt{g r_\mathrm{h} S}$ is the shear velocity, r_h is the hydraulic radius, S is the gradient of hydraulic head, which may be approximated by the gradient of the water surface or channel bed, D_{84} is the characteristic grain diameter of the surface material, for which 84 % of the material is finer, and g is gravitational acceleration. This flow resistance relation has been tested by Rickenmann and Recking (2011) based on nearly 3000 field data points. With the coefficients $a_1 = 6.5$ and $a_2 = 2.5$, it shows very good agreement with the average trend of observations, especially including the small relative flow depths with an increased flow resistance. Rickenmann and Recking (2011) rewrote Eq. (5) in an alternative version, in which flow velocity is written as a direct function of q, the discharge per unit flow width.

sedFlow allows three methods for the calculation of channel hydraulics: an explicit kinematic wave routing, an implicit kinematic wave routing and a uniform discharge approach.

The explicit flow routing corresponds to an Eulerian forward approach. In such an approach, all relevant variables are assumed constant for the duration of one time step. For numeric stability, time steps have to be short enough for this assumption to be valid. For morphodynamic simulations this may be impractical. The fast process of running water defines the short time step lengths, even though it is not the process of interest and the relatively slower morphodynamic changes would allow for much longer time steps and thus faster calculations. Except for this disadvantage, the explicit flow routing provides a routing of discharge without any restrictions concerning other concepts or parameters.

To overcome the short time steps, sedFlow also provides capabilities for implicit flow routing. Because they are unconditionally stable, implicit methods impose no requirements concerning the length of time steps. However, in implicit methods the unknown variables usually have to be found via computationally demanding iterations. In sedFlow the algorithm of Liu and Todini (2002) is implemented for solving the implicit routing. It avoids time-consuming iterations by analytically finding the solution using Taylor series approximations. However, this algorithm requires a power-law representation of discharge as a function of water volume in a reach. That means it can only be applied to infinitely deep rectangular or v-shaped channels in combination with a power-law flow resistance such as Eq. (6). Except for this restriction, the implicit flow routing provides a routing of discharge with fast computational performance.

The explicit and implicit flow routings use the bed slope as proxy for energy slope for all hydraulic and bedload transport computations. This approximation, which corresponds to the assumption of a kinematic wave, is acceptable for most mountain channels, as river bed gradients are commonly steep there. However, problems arise when tributaries deposit debris flow material in the main channel producing adverse slopes, which can occur in alpine environments. A pragmatic solution to deal with adverse slopes is the uniform discharge approach. Discharge is assumed to be equal along the entire channel, only increasing at confluences for a given time step. This procedure can be justified keeping in mind that the temporal scale of hydraulic processes is very small compared to the temporal scale of morphodynamic processes. Hydraulic calculations are performed using the bed slope proxy for the hydraulic gradient. In cases of adverse slopes, the formation of pondages is simulated. That is, flow depth and velocity are selected to ensure a minimum gradient of hydraulic head, which is positive and close to zero. For bedload transport calculations the gradient of the hydraulic head is used, which by definition can only exhibit positive slopes. Thus, the energy slope for bedload transport estimation is *not* the result of a backwater calculation, but it is the gradient

ESURFD
2, 773–822, 2014

between individual hydraulic head values, which under normal conditions have been calculated independent from each other using the local bed slope as a proxy for friction slope. It has to be noted that this approach will produce large errors, when moderate backwater effects are part of the simulated system. In such systems, the first approach, which uses bed slope both as the friction slope for the hydraulic calculations and as the energy slope for the sediment transport calculations, will produce better estimates of the transported sediment volumes, but it requires the absence of adverse channel gradients.

Partially due to the simple and efficient hydraulic schemes, several years of bedload transport and resulting slope and GSD adjustment can be simulated with sedFlow within only few hours of calculation time on a regular 2.8 GHz CPU (central processing unit) core.

Within sedFlow, the time step length used for the current time step is the minimum length obtained from three different methods of calculation for each simulated reach, as long as this minimum is smaller than a user-defined maximum time step length. When explicit or implicit kinematic wave flow routing is used, the first method ensures that local slope changes do not exceed a user-defined fraction. When explicit kinematic wave flow routing is used, the first method further calculates another time step length based on the Courant–Friedrichs–Lewy (CFL) criterion (Courant et al., 1928) for the water flow velocity multiplied by a user-defined safety factor[1]. The second method is based on the CFL criterion for the estimated bedload grain velocity multiplied by a user-defined safety factor. The third method ensures that as a maximum a user-defined fraction of the active layer is eroded.

Different formulas can be used for the estimation of bedload transport capacity. The approaches of Rickenmann (2001), Cheng (2002), Wilcock and Crowe (2003) and

[1]When explicit kinematic wave flow routing is used, the model does not check whether the calculated time step length is smaller than a user-defined maximum length, because the CFL criterion for the water flow velocity usually produces time step lengths, which are considerably smaller than commonly used maxima.

Recking (2010) are implemented in sedFlow. The formula of Rickenmann (2001) modified for fractional transport was used here:

$$\Phi_{\mathrm{bi}} = 3.1 \cdot \left(\frac{D_{90}}{D_{30}}\right)^{0.2} \cdot \sqrt{\theta_{i,\mathrm{r}}} \cdot \left(\theta_{i,\mathrm{r}} - \theta_{\mathrm{ci,\,r}}\right) \cdot \mathrm{Fr} \cdot \frac{1}{\sqrt{s-1}}; \quad \text{with} \quad q_{\mathrm{b}} = \Sigma q_{\mathrm{bi}}; \tag{7}$$

Here, $\Phi_{\mathrm{bi}} = \frac{q_{\mathrm{bi}}}{F_i\sqrt{(s-1)gD_i^3}}$ is the dimensionless bedload transport rate per grain size fraction, F_i is the relative portion compared to the total surface material with $D > 2\,\mathrm{mm}$ of a grain size fraction i with D_i as its mean diameter, q_{bi} is the volumetric bedload transport per grain size fraction and unit channel width, $s = \frac{\rho_{\mathrm{s}}}{\rho}$ is the density ratio of solids ρ_{s} and fluids ρ, Fr is the Froude number, $\theta_{\mathrm{i,\,r}} = \frac{r_{\mathrm{h}} S_{\mathrm{red}}}{(s-1)D_i}$ is the dimensionless bed shear stress and S_{red} is the reduced energy slope according to Rickenmann and Recking (2011), see also Nitsche et al. (2011). Here, D_{90} and D_{30} are characteristic grain diameters, for which 90 % or 30 % of the local grain size distribution is finer, and q_{b} is the volumetric bedload transport rate per unit channel width. The critical dimensionless bed shear stress at the initiation of transport θ_{ci} is modified by the so-called hiding function either in the form of a relatively simple power-law relation (Parker, 2008):

$$\theta_{\mathrm{ci}} = \theta_{c50} \left(\frac{D_i}{D_{50}}\right)^{m} \tag{8}$$

or in the form proposed by Wilcock and Crowe (2003):

$$\theta_{\mathrm{ci}} = \theta_{c50} \cdot \left(\frac{D_i}{D_{\mathrm{m}}}\right)^{m_{\mathrm{wc}}} \quad \text{with} \quad m_{\mathrm{wc}} = \frac{0.67}{1 + \exp\left(1.5 - \frac{D_i}{D_{\mathrm{m}}}\right)} - 1 \tag{9}$$

Here, D_{50} and D_{m} are the median and geometric mean grain diameter of surface material, m is an empiric hiding exponent and m_{wc} is the hiding exponent according to Wilcock and Crowe (2003). The empiric exponent m ranges from 0 to −1, in which

ESURFD
2, 773–822, 2014

F. U. M. Heimann et al.

-1 corresponds to equal mobility and 0 to no influence by hiding at all. The critical dimensionless bed shear stress at initiation of transport θ_{c50} is estimated based on the bed slope S_b with the empirical relation of Lamb et al. (2008) according to Eq. (10):

$$\theta_{c50} = 0.15 \cdot S_\mathrm{b}^{0.25}; \tag{10}$$

Within sedFlow a minimum value θ_cMin can be defined for θ_{c50}, as Eq. (10) results in unrealisticly low θ_{c50} values for small channel gradients. For consistency of calculations, $\theta_\mathrm{ci,\,r} = \theta_\mathrm{ci}\left(\frac{S_\mathrm{red}}{S}\right)$ is used in Eq. (7). A detailed description of sedFlow can be found in Heimann et al. (2014), in which amongst others also the sediment exchange processes between surface and sublayer are described.

2.5 Model calibration and sensitivity calculations

Using the data on channel geometry, GSD, and hydrology from the Brenno and Kleine Emme catchments, we ran the model sedFlow aiming to reproduce the observed bedload transport. The following criteria were applied to assess the agreement between simulation results and observation, which are stated in order of decreasing importance: (i) The input values such as the local GSDs should vary largely within the uncertainty range of observations. (ii) The input parameters such as the threshold bed shear stress at the beginning of bedload motion should vary within a plausible range. (iii) The simulated erosion and deposition should be as close as possible to the observed pattern. (iv) The simulated ABT should be as close as possible to the one reconstructed from field observations. (v) The GSDs at the end of the simulation should vary within a plausible range.

The calibration process consists of five steps. First, a hydraulic routing scheme is selected. Second, a bedload transport relation is selected. Third, the threshold for the initiation of motion is adjusted. Fourth, if the simple power-law hiding function of Eq. (8) is used, the exponent m is adjusted as well. Fifth, some fine-tuning is made via local reach-scale adjustments. In the first step of the calibration process of the presented

ESURFD
2, 773–822, 2014

study, the implicit kinematic wave hydraulic routing scheme was selected for the Kleine Emme, because the gentle slopes preclude the uniform discharge approach and the long simulated time period requires fast simulations. For the Brenno, the uniform discharge approach was selected, because the intense sediment inputs from the tributaries require the consideration of adverse slopes. In the fifth step of the calibration process, the reach-scale adjustments have been made to the GSD in the Kleine Emme and to the representative channel width in the Brenno river. For the Kleine Emme, the representative channel width was well constrained, while measured GSD's were relatively poorly constrained because the streambed is accessible only at a limited number of gravel bars. For the Brenno, the uncertainty about the effective channel width is relatively large along the depositional reaches in flatter areas, and for the calibration of the sedFlow simulations the mean channel width was adjusted primarily in these reaches. The corresponding simulation set-ups are summarised in Table 2.

For the Brenno the simulation of the calibration period was repeated using all three different hydraulic schemes and two flow resistance relations, which are implemented in sedFlow. Comparing these simulation results allows us to study the influence of the hydraulic algorithm on the simulated bedload transport.

To study explicitly the influence of different time step lengths, we used a set-up, in which the actual time step length generally equals the user defined maximum time step length value[2]. We compared the simulation results for different maximum time step lengths ranging from 1 min to 1 h. For any other simulation outside this time step comparison, we used a maximum time step of 15 min for the Kleine Emme and a maximum time step of 1 h for the Brenno. These two values have been selected in order to achieve reasonably short calculation times.

After the calibration exercise, the best-fit parameter set was used as base for two sensitivity studies. For the first study, in each simulation, all parameters but one are set to their original best-fit values and the remaining parameter is increased and decreased

[2]However, it cannot be excluded that in few time steps another of the conditions for temporal discretisation (listed in Sect. 2.4) caused a different time step length.

ESURFD
2, 773–822, 2014

by a certain fraction. In the following we will call this procedure a one-at-a-time range sensitivity study. We varied the parameters discharge, minimum threshold for the initiation of bedload motion θ_{cMin}, grain size and channel width by either plus or minus 30 %. Considering the more detailed knowledge of the system of the Kleine Emme, we performed additional simulations for this catchment, in which we reduced the uncertainty for discharge and channel width to plus or minus 20 %. For the second sensitivity study, all possible combinations of decreased (−30 %), best fit and increased (+30 %) values for all treated parameters were simulated[3]. In the following we will call this a complete range sensitivity study. In this complete range sensitivity analysis, the sediment input volumes from the tributaries to the Brenno were varied as well by plus or minus 30 %.

3 Results

At the Kleine Emme, simulated ABT shows agreement with the sediment budget (Fig. 6). Locally, however, simulations and observations of erosion and deposition can differ considerably. In the uppermost part down to km ∼ 17, peaks of very coarse grain size distributions are simulated. The gaps in the simulated GSD represent reaches in which the alluvial cover is washed out completely and the river runs over bedrock. Downstream of km ∼ 17, simulated final grain size distributions are close to the initial values.

At the Brenno, the simulation depicts well the interactions and qualitative transport behaviour in the vicinity of the tributaries Riale Riascio and Ri di Soi (Fig. 7). Downstream of the anthropogenic excavation at km 10, which is not considered in the simulation, the model exhibits an overall depositional trend. The low sediment transport from km 4.5 to 3 due to a locally increased channel width is well reflected in the simulations.

[3]In three simulations at the Kleine Emme with high θ_{cMin}, low discharge, coarse GSD and narrow, mean or wide channel widths, the stream could not transport the bank erosion sediment inputs near km 12. This resulted in the creation of adverse slopes. Therefore, these three simulations have been excluded from the complete range sensitivity study.

ESURFD
2, 773–822, 2014

Except for the depositional trend from km ~4.5 to km ~8 (which did not occur in the real world because substantial sediment volume was anthropogenically excavated from this reach) the simulated erosion and deposition show good agreement with the observations. In reaches with larger channel gradients the model produces a coarsening of grain size distributions. Apart from these reaches, simulated final grain size distributions are close to their initial values.

In both rivers, the model tends to smoothen differences in channel gradients (Figs. 6 and 7). The channel width is not modified during the simulations.

The simulations of the Brenno suggest an intense backward migrating erosion of the knickpoints at the confluences with debris flow tributaries, which is not observed in the field. This erosion can be prevented in the simulations either by limiting the the alluvium thickness and thus potential erosion depth, or by adding coarse blocks to the local GSD, which have not been captured in the transect pebble count, or by introducing a maximum Froude number limit in the flow resistance and drag force partitioning calculations.

In both rivers, early in the course of a simulation the model tends to adjust surface GSDs, which stay roughly the same for the rest of the simulation and which therefore seem to be stable under the local conditions (i.e. local slope, channel width, subsurface GSD and discharge pattern).

In the Kleine Emme, the variation of maximum time step length caused differences in the modelled erosion and deposition only at few locations. This results in small differences in modelled ABT along the complete river length (Fig. 10). In the Brenno, long maximum time step lengths caused an underestimation of the depositional trend from km 6 to 5. Downstream of this position, the underestimated deposition resulted in an overestimation of simulated ABT (Fig. 11).

3.1 Sensitivity analyses

The local sensitivity analysis (Fig. 8) shows that variations in input discharge and GSDs have a large influence on the resulting ABT in both rivers. The impact of variations of the

ESURFD
2, 773–822, 2014
Recalculation of bedload transport observations
F. U. M. Heimann et al.

minimum value for the threshold dimensionless shear stress at the initiation of bedload motion θ_{cMin} ranges from low in the Brenno to high in the Kleine Emme. In general, relative output variations are larger in the Kleine Emme as compared to the Brenno. However, this trend is less pronounced for the simulations with reduced uncertainty at the Kleine Emme.

Comparing the three implemented hydraulic schemes, the explicit and implicit hydraulic flow routing produce practically identical results and the differences to using an uniform discharge approach are small in the Brenno catchment (Fig. 9). In contrast, there is a considerable difference in ABT between the simulations when using the two different flow resistance relations (Fig. 9).

As a main result of the complete range sensitivity study, the complete variation of input values caused considerable variation in the simulated ABT, but caused very little variability in the simulated erosion and deposition (Figs. 12 and 13).

4 Discussion

4.1 Simulations for the calibration period

Bedload transport and morphodynamic observation of both rivers can be reproduced with reasonable parameter set-ups (Table 2 and Figs. 6 and 7). At the Kleine Emme the simulated absolute values of net erosion and net deposition at the end of the calibration period are small and thus close to the noise of the measurements. Therefore, the differences between observed and simulated morphodynamics may be partly explained as noise. The simulated peaks of very coarse GSD in the upper part of the Kleine Emme are due to the thin alluvium thickness, which is in some places washed out completely or almost completely. If only a few coarse grains are left in a reach, they will produce exremely coarse grain size percentiles. At the Brenno, the deposition from km ~ 4.5 to km ~ 8 (Fig. 7), which substitutes for the unconsidered excavation, appears as a plausible behaviour of the river without any anthropogenic interventions.

Discussion Paper | Discussion Paper | Discussion Paper | Discussion Paper |

ESURFD

2, 773–822, 2014

Recalculation of bedload transport observations

F. U. M. Heimann et al.

Coarsening at reaches with increased channel gradient is plausible as well. At the Brenno, the minimum threshold dimensionless shear stress θ_{cMin} for the initiation of bedload motion has been calibrated to a value of 0.1 (Table 2). This corresponds to the findings of Lamb et al. (2008) and Bunte et al. (2013), who showed that in mountain rivers θ_{c} may well assume values in this order of magnitude.

The good agreement of bedload transport simulations and observations may be surprising, given that the natural system is complex and the model representation is relatively simple, with only a few parameters for calibration. The selected transport equation and threshold for the initiation of motion determines the average level of transport volumes. The selected hiding function locally modulates the calculated volumes and in particular influences the evolution of the GSD. Despite its simplicity, the described modelling framework appears to be adequate for a quantitative description of bedload transport processes, as suggested by the reasonable agreement of simulation and observation.

The better agreement of simulated and reference ABT at the Kleine Emme compared to the Brenno is not surprising. At the Kleine Emme, there are no debris flow inputs, the influence of tributaries is limited and the sediment outflow is well known. The Kleine Emme is a well-defined system with low uncertainties and thus ideal for simulation. In addition, spatially distributed calibration was applied more extensively to the Kleine Emme as compared to the Brenno. For the Brenno, spatially distributed calibration was performed by adjusting the width of the channel. This was done only at depositional reaches, which entail considerable uncertainty concerning the representative substitute channel width and which correspond to only ca. 30 % of the total study reach. In contrast, at the Kleine Emme, spatially distributed calibration was performed by adjusting local GSDs along the *complete* study reach. This more extensive, spatially distributed calibration at the Kleine Emme partly also explains the better agreement of simulated and reference ABT at the Kleine Emme compared to the Brenno.

Few studies (Lopez and Falcon, 1999; Chiari and Rickenmann, 2011; Mouri et al., 2011) have performed a spatially distributed comparison of simulations and field observations, similar to what is presented in this article. However, these studies focused on shorter river lengths than the Brenno and the Kleine Emme. Lopez and Falcon (1999) performed a lumped calibration by simply multiplying calculated transport rates by four. In all aforementioned studies, the models have been calibrated but not independently validated (similarly to the present investigation). This contrasts with approaches used in other research fields such as hydrology (Beven and Young, 2013), where it is common practice to perform a calibration and a validation separately. The lack of independent validation is mainly due to the marked scarcity of available field data on bedload transport. Other studies compared simulation results against point data derived from field observations (Hall and Cratchley, 2006; Li et al., 2008), against analytic considerations (García-Martinez et al., 2006) or against a combination of field data and analytical results along with additional flume experiment data and results from other models (Papanicolaou et al., 2004). Many studies discuss model behaviour without any explicit comparison between that behaviour and observational data (Lopez and Falcon, 1999; Papanicolaou et al., 2004; Hall and Cratchley, 2006; Li et al., 2008; García-Martinez et al., 2006; Radice et al., 2012).

The simulated GSDs might be seen as a proxy for GSDs, which are consistent with local slope, channel geometry and discharge pattern. This idea is rather attractive, as the model would use variables with a low uncertainty to estimate the local GSD, which is associated with a relatively large uncertainty. Unfortunately, the simulated surface GSD also depends on the subsurface GSD, and on the algorithm regulating the exchange between the surface and subsurface layers (for details see Heimann et al., 2014). In other terms, the simulated surface GSD is either consistent with local conditions and an unrealistically small interaction between surface and subsurface or it is consistent with local conditions and a highly uncertain and possibly incorrect subsurface GSD. Nevertheless, these simulated GSDs will be internally consistent with the other assumptions in the model and thus may have the potential to serve as input for calibration exercises and follow-up studies. A detailed investigation of this topic is beyond the scope of this article.

ESURFD

2, 773–822, 2014

Recalculation of bedload transport observations

F. U. M. Heimann et al.

The simulated erosion of knickpoints in the Brenno was not observed in the field and is thus unrealistic. This suggests that large blocks, which are present in these reaches, but which have not been captured by the transect pebble counts, are important to stabilise the bed. The influence of large blocks also explains why the GSD at these positions had to be coarsened to achieve realistic model behaviour. In addition, the simulated GSDs coarsened even further. Both the unrealistic erosion and the need for coarsened GSDs point to the limitations of a volumetric percentile grain diameter to serve as a proxy for channel roughness. Flow resistance estimation in the Manning–Strickler and in the variable power equation formulation (Ferguson, 2007) depends on the representative grain diameter D_{84}. However, even a few large blocks, possibly at percentiles higher than 84, can heavily influence the properties of flow. The problems of a single representative grain size percentile used as a proxy for bed roughness become more severe in the case of a discontinuous GSD, for example if the coarse blocks originate from rock fall and thus from a different source as the alluvial gravel. In such cases, any percentile diameter will considerably over- or underestimate the roughness, if its value falls in the gap of the GSD. Coarse blocks are also a problem for the general concept of a volumetric percentile. Only a small fraction of the volume of a large block belongs to the surface layer of the river bed, which is assumed to define its roughness. Large parts of the block protrude into the deeper alluvium or into the water flow not belonging to the surface layer. Therefore the volumetric contribution of such blocks to the surface layer is hard to determine. The described issues are reflected in conceptual models for flow resistance like the ones of Yager et al. (2007) or Nitsche et al. (2012), which consider large blocks explicitly e.g. in terms of a surface block density. In a recent study Ghilardi (2013) suggested that the protrusion height of large blocks into the flow could be used as a potential proxy for flow resistance. Based on this approach, the visual appearance of the Brenno river bed (Fig. 14) suggests a roughness of about one to two meters. This value is of the same order of magnitude as the D_{84} of the coarsened GSDs (Fig. 7), which we used as a roughness proxy in our simulations. It is further supported by additional area block counts in the Brenno,

ESURFD
2, 773–822, 2014

Recalculation of bedload transport observations

F. U. M. Heimann et al.

which showed that grains with a diameter smaller than 1 m only make up 90 % of the surface layer's sediment volume or even only 75 % at the confluence with the Riale Riascio. These blocks observed in the field dominate the macro-roughness. Since D_{84} is selected to represent macro-roughness, the block counts support the D_{84} values which are used in the simulations, and which are in the same order of magnitude as the observed block diameters. Of course, the problems related to discontinuous GSDs and the uncertain volumetric contribution of blocks to a surface layer have to be considered in this context.

To assess the influence of time step length, the user-defined maximum time step length was varied between 1 min and 1 h. In the Kleine Emme, the influence of time step length is negligible compared to the overall uncertainty of bedload transport simulations (Fig. 10). In the Brenno, the effect of large maximum time step lengths is spatially limited and well defined (Fig. 11) and thus can be easily considered in the interpretation of the simulation results.

4.2 Sensitivity analyses

The limitations of simple one-at-a-time sensitivity studies for the analysis of non-linear processes are well known (Saltelli et al., 2006). However, an adequate global sensitivity analysis, in which the complete parameter space is covered, would go beyond the scope of this article.

As shown in Fig. 8 the model reacts differently to input changes, depending on which parameter is changed. The model's reaction to input changes also depends on the current river setting. For example, the relative variability and thus uncertainty of model outputs is generally larger in the Kleine Emme as compared to the Brenno. This may be partially due to the fact that the volumes of transported sediment are generally smaller in the Kleine Emme as compared to the Brenno. However, the output uncertainty can be partially compensated by a better supported knowledge and thus higher confidence in the inputs (dotted lines in Fig. 8). Interestingly, even the order of parameter sensitivities may change depending on the current river setting. For example, the reaction

ESURFD
2, 773–822, 2014

Recalculation of bedload transport observations

F. U. M. Heimann et al.

to changes in the minimum threshold for the initiation of bedload transport θ_{cMin} differs considerably for the two rivers. In the Kleine Emme, the uncertainty of this parameter seems to be responsible for a large part of the model output uncertainty. In contrast in the Brenno, θ_{cMin} plays a rather subordinate role.

In the complete range sensitivity study (Figs. 12 and 13) all input variations have been applied to the complete length of the river. This may explain why the simulated erosion and deposition show only limited variation compared to the simulated ABT. Erosion and deposition are a function of gradual changes of channel properties (gradient, width, GSD, inputs) along the river. Applying the input variation to the complete length of the river keeps the relative changes of channel properties the same. Even though bedload transport is not a linear system, the input variation on the complete length of the river did not cause considerable variation of simulated erosion and deposition. Nevertheless, the sensitivity study with its highly variable ABT and almost constant morphodynamics stresses the uncertainty of ABT that is only derived from morphologic changes. These simulation results support previous studies which have discussed this uncertainty (Kondolf and Matthews, 1991; Reid and Dunne, 2003; Erwin et al., 2012). This is especially important because ABT plots are very common for the description of bedload transport in applied engineering practice and are even recommended by authorities (e.g., Schälchli and Kirchhofer, 2012).

As is illustrated in Fig. 9 for the Brenno river, the two different flow resistance relations produce considerably different values of simulated ABT. This further stresses the limitations of Manning–Strickler type flow resistance relations in steep mountain streams as discussed in Rickenmann and Recking (2011). In contrast, the three different hydraulic schemes predict similar transported bedload volumes in the Brenno River (Fig. 9). Differences can be neglected when compared to the overall uncertainties of bedload transport simulations. Therefore, the influence on the model outputs does not constitute a preference for any of the hydraulic schemes and any scheme can be selected based on its characteristics. If adverse slopes may occur or if the variable power equation flow resistance, which is more suitable for shallow flow in steeper

ESURFD
2, 773–822, 2014

Recalculation of bedload transport observations

F. U. M. Heimann et al.

channels, shall be used without slowing down the calculations, one may select the uniform discharge approach. If neither the ability to deal with adverse slopes nor the use of the variable power equation flow resistance is required, one may select the implicit kinematic wave routing, as it provides a real routing of discharge. If a variable power equation approach shall be combined with a routing of discharge, one may select the explicit kinematic wave routing, even though this option is not recommended due to its long calculation times.

5 Conclusions

In this article, we used the model sedFlow to recalculate bedload transport observations in two Swiss mountain rivers. sedFlow is a tool designed for the simulation of bedload dynamics in mountain streams. Observations from bedload transport events have been successfully reproduced with reasonable parameter settings. The results of the one-at-a-time range sensitivity analysis have shown that a defined change of an input parameter produces larger relative changes of output sediment transport rates in the Kleine Emme as compared to the Brenno, which may be due to the generally smaller transport rates at the Kleine Emme. Simulation results highlighted the problems that can arise because traditional flow resistance estimation methods fail to account for the influence of large blocks. As an important result of our study, we conclude that a very detailed and sophisticated representation or hydraulic processes is apparently not necessary for a good representation of bedload transport processes in steep mountain streams. Both uniform flow routing and kinematic wave routing performed well in simulating field observations related to bedload transport. Moreover, it has been shown that bedload transport events with widely differing accumulated bedload transport (ABT) may produce identical patterns of erosion and deposition. This highlights the uncertainty in ABT estimates that are derived only from morphologic changes. This proof-of-concept study demonstrates the usefulness of sedFlow for a range of practical applications in alpine mountain streams.

ESURFD
2, 773–822, 2014

Acknowledgements. We are greatful to Christa Stephan (project thesis ETH/WSL), Lynn Burkhard (MSc thesis ETH/WSL), Anna Pöhlmann (WSL), Claudia Bieler (MSc thesis ETH/WSL) and Christian Greber (MSc thesis ETH/WSL) for their contributions to the development and application of sedFlow. Special thanks to Massimiliano Zappa for his PREVAH support and the hydrologic input data. We thank the Swiss National Science Foundation for funding of this work in the framework of the NRP 61 project "Sedriver" (SNF grant no. 4061-125975/1/2). The simulations in the Brenno river were also supported by the BAFU (GHO) project "Feststofftransport in Gebirgs-Einzugsgebieten" (contract no. 11.0026.PJ/K154-7241) of the Swiss Federal Office for the Environment.

References

Bathurst, J. C., Bovolo, C. I., and Cisneros, F.: Modelling the effect of forest cover on shallow landslides at the river basin scale, Ecol. Eng., 36, 317–327, doi:10.1016/j.ecoleng.2009.05.001, 2010. 775

Beffa, C.: 2D-Simulation der Sohlenreaktion in einer Flussverzweigung, Österreichische Wasser- und Abfallwirtschaft, 42, 1–6, 2005. 775

Beven, K. and Young, P.: A guide to good practice in modeling semantics for authors and referees, Water Resour. Res., 49, 5092–5098, doi:10.1002/wrcr.20393, 2013. 795

Bhowmik, N. G., Tsai, C., Parmar, P., and Demissie, M.: Case study: application of the HEC-6 model for the main stem of the Kankakee River in Illinois, J. Hydraul. Eng.-ASCE, 134, 355–366, doi:10.1061/(ASCE)0733-9429(2008)134:4(355), 2008. 775

Bunte, K., Abt, S. R., Potyondy, J. P., and Swingle, K. W.: A comparison of coarse bedload transport measured with bedload traps and Helley–Smith samplers, Geodin. Acta, 21, 53–66, doi:10.3166/ga.21.53-66, 2008. 775

Bunte, K. B., Abt, S. R., Swingle, K. W., Cenderelli, D. A., and Schneider, J. M.: Critical Shields values in coarse-bedded steep streams, Water Resour. Res., 49, 1–21, doi:10.1002/2012WR012672, 2013. 776, 794

Cheng, N.-S.: Exponential formula for bedload transport, J. Hydraul. Eng.-ASCE, 128, 942–946, doi:10.1061/(ASCE)0733-9429(2002)128:10(942), 2002. 787

ESURFD

2, 773–822, 2014

Recalculation of bedload transport observations

F. U. M. Heimann et al.

Chiari, M. and Rickenmann, D.: Back-calculation of bedload transport in steep channels with a numerical model, Earth Surf. Proc. Land., 36, 805–815, doi:10.1002/esp.2108, 2011. 776, 794

Chiari, M., Friedl, K., and Rickenmann, D.: A one-dimensional bedload transport model for steep slopes, J. Hydraul. Res., 48, 152–160, doi:10.1080/00221681003704087, 2010. 775, 782

Courant, R., Friedrichs, K., and Lewy, H.: Über die partiellen Differenzengleichungen der mathematischen Physik, Math. Ann., 100, 32–74, doi:10.1007/BF01448839, 1928. 787

Doten, C. O., Bowling, L. C., Lanini, J. S., Maurer, E. P., and Lettenmaier, D. P.: A spatially distributed model for the dynamic prediction of sediment erosion and transport in mountainous forested watersheds, Water Resour. Res., 42, W04417, doi:10.1029/2004WR003829, 2006. 775

Erwin, S. O., Schmidt, J. C., Wheaton, J. M., and Wilcock, P. R.: Closing a sediment budget for a reconfigured reach of the Provo River, Utah, United States, Water Resour. Res., 48, W10512, doi:10.1029/2011WR011035, 2012. 798

Faeh, R., Mueller, R., Rousselot, P., Vetsch, D., Volz, C., Vonwiller, L., Veprek, R., and Farshi, D.: System manuals of BASEMENT. vol 2.2., VAW, ETH Zurich, Switzerland, available at: www.basement.ethz.ch (last access: 15 July 2014), 2011. 775

Fehr, R.: Einfache Bestimmung der Korngrössenverteilung von Geschiebematerial, Schweizer Ingenieur und Architekt, 105, 1104–1109, 1987. 783

Ferguson, R.: Flow resistance equations for gravel- and boulder-bed streams, Water Resour. Res., 43, W05427, doi:10.1029/2006WR005422, 2007. 784, 796

Ferguson, R. I., Church, M., and Weatherly, H.: Fluvial aggradation in Vedder River: Testing a one-dimensional sedimentation model, Water Resour. Res., 37, 3331–3347, doi:10.1029/2001WR000225, 2001. 775

Flussbau AG: Geschiebetransport im Brenno. Einfluss der Murgangablagerung aus dem Ri di Soi, Tech. rep., Reppublica e Cantone Ticino – Divisione delle costruzioni – Ufficio dei corsi d'acqua, 2003. 781, 806

Flussbau AG: Revitalisierung von Auenökosystemen (Risanamento dei Ecosistemi Alluvionali) Fachbericht Morphologie und Geschiebe, Tech. rep., Reppublica e Cantone Ticino – Dipartimento del Territorio – Consorzio Risanamento Ecosistemi Alluvionali, 2005. 781, 806

Flussbau AG: Ereignisanalyse Hochwasser 2005 – Seitenerosion, Tech. rep., Swiss Federal Office for the Environment FOEN, 2009. 781

García-Martinez, R., Espinoza, R., Valeraa, E., and González, M.: An explicit two-dimensional finite element model to simulate short- and long-term bed evolution in alluvial rivers, J. Hydraul. Res., 44, 755–766, doi:10.1080/00221686.2006.9521726, 2006. 775, 795

Geoportal Kanton Luzern: available at: www.geo.lu.ch/map/gewaessernetz (last access: 27 August 2013), 2013. 778

Ghilardi, T.: Intense sediment transport and flow conditions in steep mountain rivers considering the large immobile boulders, Ph.D. thesis, École polytechnique fédérale de Lausanne, 2013. 796

Gray, J. R., Laronne, J. B., and Marr, J. D.: Bedload-Surrogate Monitoring Technologies, Tech. rep., US Geological Survey Scientific Investigations Report 2010-5091, available at: http://pubs.usgs.gov/sir/2010/5091 (last access: 15 July 2014), 2010. 775

Habersack, H., Hengl, M., Huber, B., Lalk, P., and Tritthart, M. (Eds.): Fließgewässermodellierung – Arbeitsbehelf Feststofftransport und Gewässermorphologie, Austrian Federal Ministry of Agriculture, Forestry, Environment and Water Management and Österreichischer Wasser- und Abfallwirtschaftsverband ÖWAV, Vienna, 2011. 774

Hall, G. and Cratchley, R.: Sediment erosion, transport and deposition during the July 2001 Mawddach extreme flood event, in: Sediment Dynamics and the Hydromorphology of Fluvial Systems, Dundee, UK, July, 136–147, 2006. 775, 795

Heimann, F. U. M., Rickenmann, D., Turowski, J. M., and Kirchner, J. W.: sedFlow – an efficient tool for simulating bedload transport, bed roughness, and longitudinal profile evolution in mountain streams, Earth Surf. Dynam. Discuss., 2, 733–772, doi:10.5194/esurfd-2-733-2014, 2014. 776, 784, 789, 795

Hunziker, Zarn & Partner AG: Kleine Emme, Geschiebehaushaltstudie. Abschnitt Fontanne bis Reuss, Tech. rep., by order of Kanton Luzern Dienststelle Verkehr und Infrastruktur, Aarau, Switzerland, 2009. 781

Hunzinger, L. and Krähenbühl, S.: Sohlenveränderungen und Geschiebefrachten, in: Ereignisanalyse Hochwasser 2005. Teil 2 – Analyse von Prozessen, Massnahmen und Gefahrengrundlagen, edited by: Bezzola, G. R. and Hegg, C., Swiss Federal Office for the Environment FOEN and Swiss Federal Research Institute WSL, Chap. 4.2, 118–125, Berne, Switzerland, 2008. 781

Kondolf, G. M. and Matthews, W. V. G.: Unmeasured residuals in sediment budgets: a cautionary note, Water Resour. Res., 27, 2483–2486, doi:10.1029/91WR01625, 1991. 798

Lamb, M. P., Dietrich, W. E., and Venditti, J. G.: Is the critical Shields stress for incipient sediment motion dependent on channel-bed slope?, J. Geophys. Res., 113, F02008, doi:10.1029/2007JF000831, 2008. 776, 789, 794

Li, S., Millar, R., and Islam, S.: Modelling gravel transport and morphology for the Fraser River Gravel Reach, British Columbia, Geomorphology, 95, 206–222, doi:10.1016/j.geomorph.2007.06.010, 2008. 775, 795

Liu, Z. and Todini, E.: Towards a comprehensive physically-based rainfall-runoff model, Hydrol. Earth Syst. Sci., 6, 859–881, doi:10.5194/hess-6-859-2002, 2002. 786

Lopez, J. L. and Falcon, M. A.: Calculation of bed changes in mountain streams, J. Hydraul. Eng.-ASCE, 125, 263–270, doi:10.1061/(ASCE)0733-9429(1999)125:3(263), 1999. 775, 794, 795

Lukey, B., Sheffield, J., Bathurst, J., Hiley, R., and Mathys, N.: Test of the SHETRAN technology for modelling the impact of reforestation on badlands runoff and sediment yield at Draix, France, J. Hydrol., 235, 44–62, doi:10.1016/S0022-1694(00)00260-2, 2000. 775

Mouri, G., Shiiba, M., Hori, T., and Oki, T.: Modeling reservoir sedimentation associated with an extreme flood and sediment flux in a mountainous granitoid catchment, Japan, Geomorphology, 125, 263–270, doi:10.1016/j.geomorph.2010.09.026, 2011. 775, 794

Nitsche, M., Rickenmann, D., Turowski, J. M., Badoux, A., and Kirchner, J. W.: Evaluation of bedload transport predictions using flow resistance equations to account for macro-roughness in steep mountain streams, Water Resour. Res., 47, W08513, doi:10.1029/2011WR010645, 2011. 776, 788

Nitsche, M., Rickenmann, D., Kirchner, J. W., Turowski, J. M., and Badoux, A.: Macroroughness and variations in reach-averaged flow resistance in steep mountain streams, Water Resour. Res., 48, W12518, doi:10.1029/2012WR012091, 2012. 796

Papanicolaou, A. N., Bdour, A., and Wicklein, E.: One-dimensional hydrodynamic/sediment transport model applicable to steep mountain streams, J. Hydraul. Res., 42, 357–375, doi:10.1080/00221686.2004.9641204, 2004. 775, 795

Parker, G.: Transport of gravel and sediment mixtures, in: Sedimentation Engineering: Theories, Measurements, Modeling, and Practice, vol. 110 of ASCE Manuals and Reports on Engineering Practice, American Society of Civil Engineers (ASCE), Chap. 3, 165–252, 2008. 776, 782, 788

ESURFD
2, 773–822, 2014

Recalculation of bedload transport observations

F. U. M. Heimann et al.

Radice, A., Giorgetti, E., Brambilla, D., Longoni, L., and Papini, M.: On integrated sediment transport modelling for flash events in mountain environments, Acta Geophys., 60, 191–2013, doi:10.2478/s11600-011-0063-8, 2012. 795

Recking, A.: A comparison between flume and field bed load transport data and consequences for surface-based bed load transport prediction, Water Resour. Res., 46, W03518, doi:10.1029/2009WR008007, 2010. 776, 788

Recking, A.: Simple method for calculating reach-averaged bed-load transport, J. Hydraul. Eng.-ASCE, 139, 70–75, doi:10.1061/(ASCE)HY.1943-7900.0000653, 2013. 776

Reid, L. M. and Dunne, T.: Sediment budgets as an organizing framework in fluvial geomorphology, in: Tools in Fluvial Geomorphology, edited by: Kondolf, G. M. and Piégay, H., John Wiley and Sons, Ltd., Chap. 16, 463–500, 2003. 798

Rickenmann, D.: Comparison of bed load transport in torrent and gravel bed streams, Water Resour. Res., 37, 3295–3305, doi:10.1029/2001WR000319, 2001. 776, 787, 788

Rickenmann, D.: Alluvial steep channels: flow resistance, bedload transport prediction, and transition to debris flows, in: Gravel Bed Rivers: Processes, Tools, Environment, edited by: Church, M., Biron, P. M., and Roy, A. G., John Wiley & Sons, 386–397, Chichester, UK, 2012. 776

Rickenmann, D. and Recking, A.: Evaluation of flow resistance in gravel-bed rivers through a large field data set, Water Resour. Res., 47, W07538, doi:10.1029/2010WR009793, 2011. 776, 785, 788, 798

Saltelli, A., Ratto, M., Tarantola, S., Campolongo, F., European Commission, and Joint Research Centre of Ispra (I): Sensitivity analysis practices: strategies for model-based inference, Reliab. Eng. Syst. Safe., 91, 1109–1125, doi:10.1016/j.ress.2005.11.014, 2006. 797

Schälchli, U. and Kirchhofer, A.: Sanierung Geschiebehaushalt. Strategische Planung. Ein Modul der Vollzugshilfe Renaturierung der Gewässer, Swiss Federal Office for the Environment FOEN, Berne, Switzerland, 2012. 798

Stricker, B.: Murgänge im Torrente Riascio (TI): Ereignisanalyse, Auslösefaktoren und Simulation von Ereignissen mit RAMMS, M.S. thesis, University of Zurich and Swiss Federal Research Institute WSL, 2010. 781, 806

Turowski, J. M., Badoux, A., and Rickenmann, D.: Start and end of bedload transport in gravel-bed streams, Geophys. Res. Lett., 38, L04401, doi:10.1029/2010GL046558, 2011. 776

ESURFD
2, 773–822, 2014

Viviroli, D., Zappa, M., Gurtz, J., and Weingartner, R.: An introduction to the hydrological modelling system PREVAH and its pre- and post-processing-tools, Environ. Modell. Softw., 24, 1209–1222, doi:10.1016/j.envsoft.2009.04.001, 2009. 779

Wicks, J. and Bathurst, J.: SHESED: a physically based, distributed erosion and sediment yield component for the SHE hydrological modelling system, J. Hydrol., 175, 213–238, doi:10.1016/S0022-1694(96)80012-6, 1996. 775

Wilcock, P. R. and Crowe, J. C.: Surface-based transport model for mixed-size sediment, J. Hydraul. Eng.-ASCE, 129, 120–128, doi:10.1061/(ASCE)0733-9429(2003)129:2(120), 2003. 776, 787, 788, 807, 808

Yager, E. M., Kirchner, J. W., and Dietrich, W. E.: Calculating bed load transport in steep boulder bed channels, Water Resour. Res., 43, W07418, doi:10.1029/2006WR005432, 2007. 796

ESURFD

2, 773–822, 2014

Recalculation of bedload transport observations

F. U. M. Heimann et al.

ESURFD
2, 773–822, 2014

Recalculation of bedload transport observations

F. U. M. Heimann et al.

Table 1. Estimated sediment input yields from tributaries to the Brenno (based on Flussbau AG, 2003, 2005; Stricker, 2010) (Process types: DF = debris flow, FT = fluvial bedload transport).

Tributary	Type	Per year [$m^3\,a^{-1}$]			1999–2009 [m^3]		
		Min.	Mean	Max.	Min.	Mean	Max.
Brenno della Greina	FT	2500		7500	25 000		75 000
Brenno del Lucomagno/Ri di Piera	FT	1500		5000	15 000		50 000
Riale Riascio	DF	4000	10 000	22 000	40 000	100 000	220 000
Ri di Soi	DF + FT	10 000	20 000	30 000	100 000	200 000	300 000
Lesgiüna	FT	1000	2000	5000	10 000	20 000	50 000
Crenone (Vallone)	DF	1000	1500	4000	10 000	15 000	40 000

Table 2. Summary of calibration period simulations with different equation sets.

Figure	River	Flow Resistance	Bedload Transport	Threshold for Transport	ABT-RMSE	ABT-Nash–Sutcliffe
6	Kleine Emme	Manning–Strickler-Type	Rickenmann W and C hiding*	Lamb et al. $\theta_{cMin} = 0.06$	7.83 10^3 m^3	0.949
7	Brenno	Variable power-law	Rickenmann No hiding	Lamb et al. $\theta_{cMin} = 0.1$	18.0 10^3 m^3	0.733

* Wilcock and Crowe (2003) hiding (Eq. 9).

ESURFD

2, 773–822, 2014

Table A1. Notation.

The following symbols are used in this article	
η_{pore}	= pore volume fraction
θ_i	= dimensionless bed shear stress for ith grain size fraction
$\theta_{i,\mathrm{r}}$	= θ_i using S_{red} to account for macro-roughness
θ_c	= dimensionless bed shear stress at initiation of bedload motion
θ_{ci}	= θ_c for ith grain size fraction
θ_{c50}	= θ_c for the median grain diameter
θ_{cMin}	= minimum value for θ_{c50}
$\theta_{\mathrm{ci,\,r}}$	= θ_{ci} accounting for macro-roughness
ρ	= fluid density
ρ_{s}	= sediment density
Φ_{bi}	= dimensionless bedload flux for ith grain size fraction
a_1, a_2	= empiric constants
D_i	= mean grain diameter for ith grain size fraction
D_{m}	= geometric mean for grain diameters
D_x	= xth percentile for grain diameters
D_{50}	= median grain diameter
F_i	= proportion of ith grain size fraction
Fr	= Froude number
g	= gravitational acceleration
m	= empiric hiding exponent ranging from 0 to −1
m_{wc}	= hiding exponent according to Wilcock and Crowe (2003)
q	= discharge per unit flow width
Q_{b}	= bedload flux
q_{b}	= bedload flux per unit flow width
q_{bi}	= q_b for ith grain size fraction
$q_{\mathrm{b_{lat}}}$	= lateral bedload influx per unit flow width
q_c	= threshold q for initiation of bedload motion
r_{h}	= hydraulic radius
s	= density ratio of solids and fluids
S	= slope of hydraulic head
S_{b}	= slope of river bed
S_{red}	= slope reduced for macro-roughness
t	= time
v_m	= average flow velocity
v^*	= shear velocity
V_{cap}	= volume of sediment corresponding to the transport capacity in a reach
V_{EroDepo}	= volume of sediment that is eroded or deposited in a reach
V_{in}	= volume of sediment that enters a reach
V_{inUp}	= volume of sediment that enters a reach from upstream
V_{inLat}	= volume of sediment that is introduced laterally to a reach
V_{out}	= volume of sediment that exits a reach
x	= distance in flow direction
z	= elevation of channel bed

ESURFD
2, 773–822, 2014

Recalculation of bedload transport observations

F. U. M. Heimann et al.

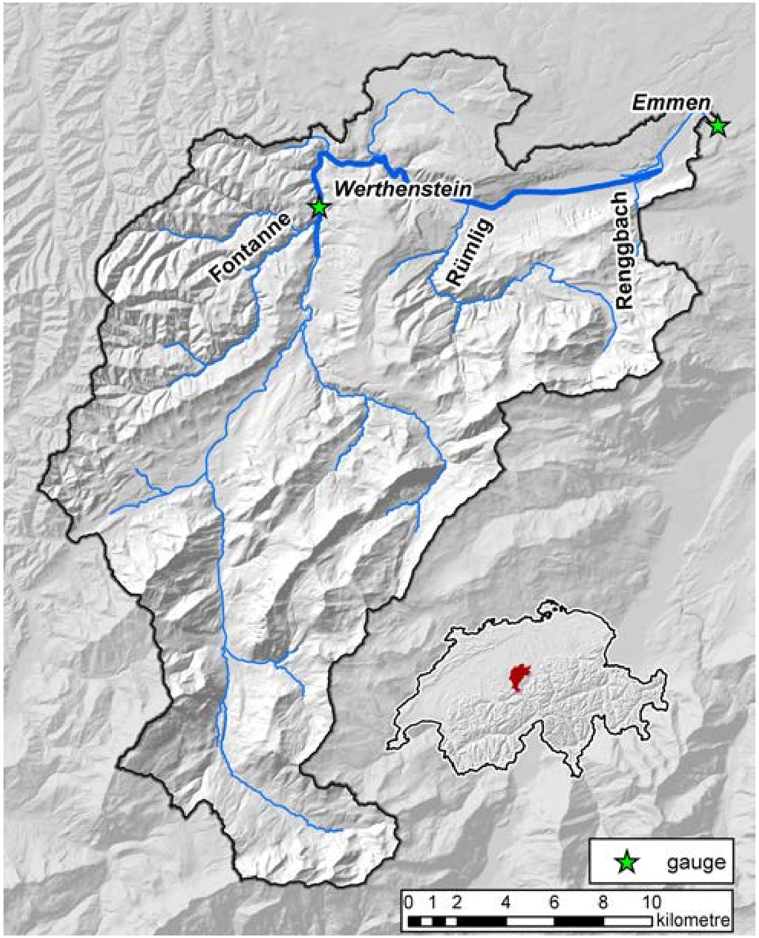

Figure 1. The Kleine Emme catchment in central Switzerland. The study reach from Doppleschwand to the confluence with the Renggbach is indicated by the bold blue line.

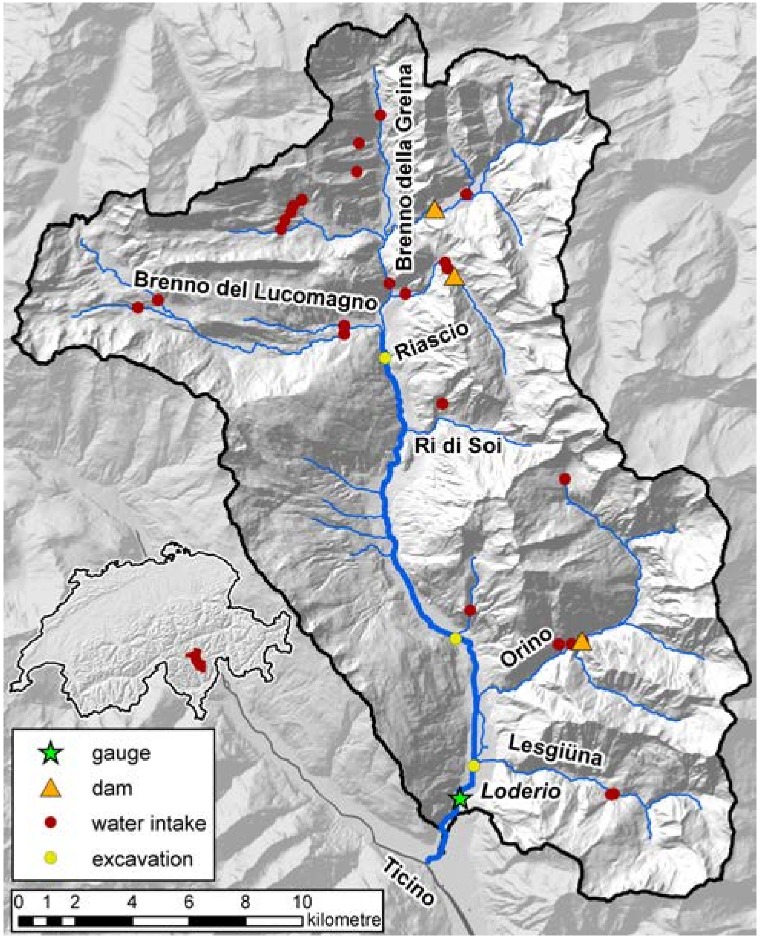

Figure 2. The Brenno catchment in southern Switzerland. The study reach from Olivone to Biasca is indicated by the bold blue line.

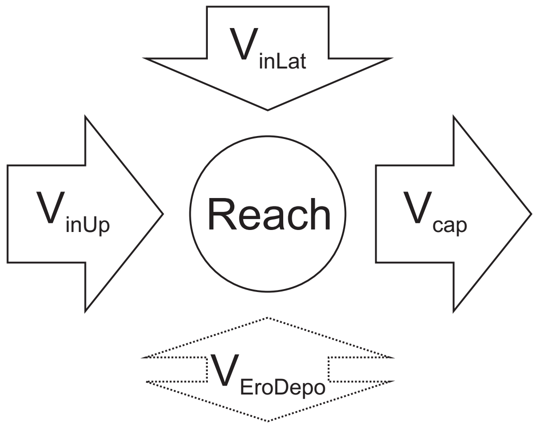

Figure 3. Schematic visualisation of Eqs. (2) to (4).

Discussion Paper | Discussion Paper | Discussion Paper | Discussion Paper |

ESURFD

2, 773–822, 2014

Recalculation of bedload transport observations

F. U. M. Heimann et al.

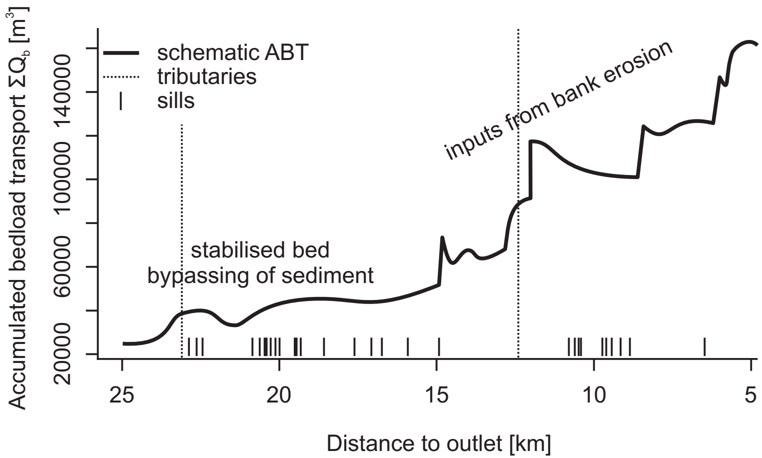

Figure 4. Commented schematic representation of accumulated bedload transport (ABT) in the Kleine Emme. (Tributaries from up- to downstream: Fontanne, Rümlig)

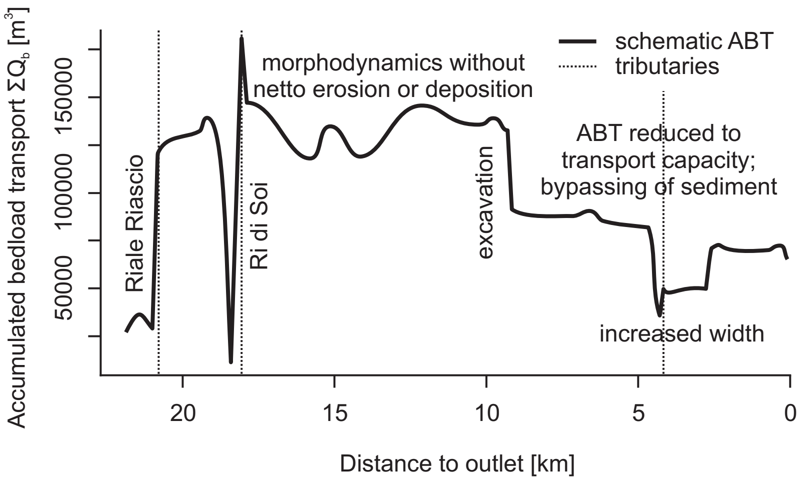

Figure 5. Commented schematic representation of accumulated bedload transport (ABT) in the Brenno. (Tributaries from up- to downstream: Riale Riascio, Ri di Soi, Lesgiüna)

ESURFD
2, 773–822, 2014

Recalculation of bedload transport observations

F. U. M. Heimann et al.

Title Page
Abstract Introduction
Conclusions References
Tables Figures
Back Close
Full Screen / Esc
Printer-friendly Version
Interactive Discussion

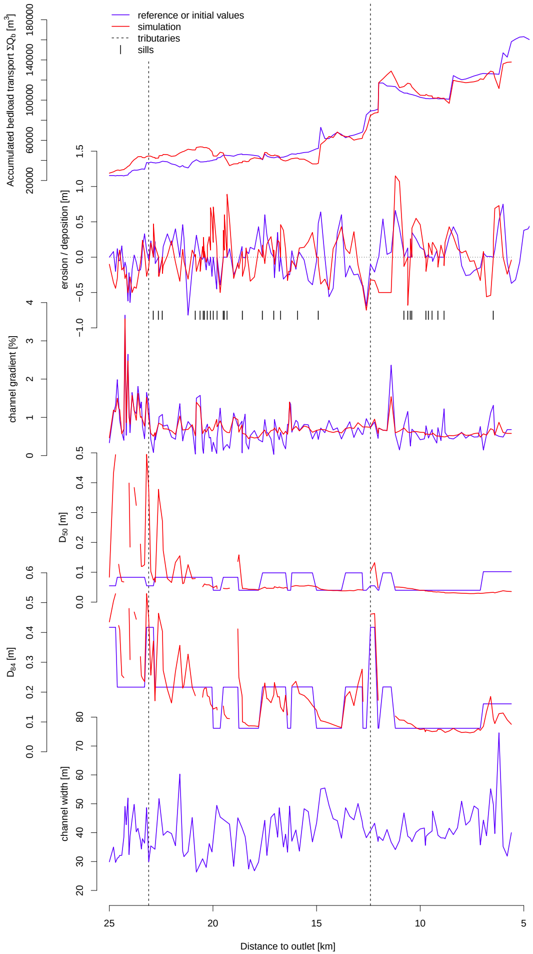

Figure 6. Comparison of predictions and observations related to bedload transport in the Kleine Emme for the period 2000–2005 (tributaries from up- to downstream: Fontanne, Rümlig).

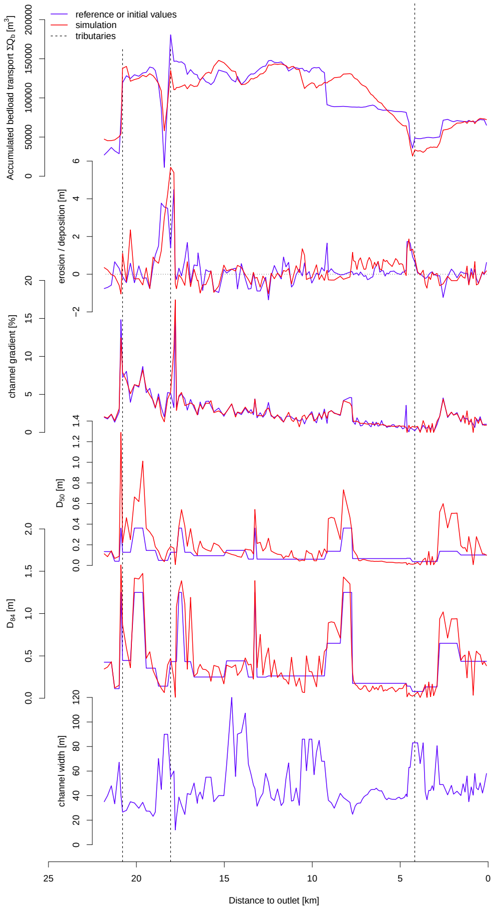

Figure 7. Comparison of predictions and observations related to bedload transport in the Brenno for the period 1999–2009 (tributaries from up- to downstream: Riale Riascio, Ri di Soi, Lesgiüna).

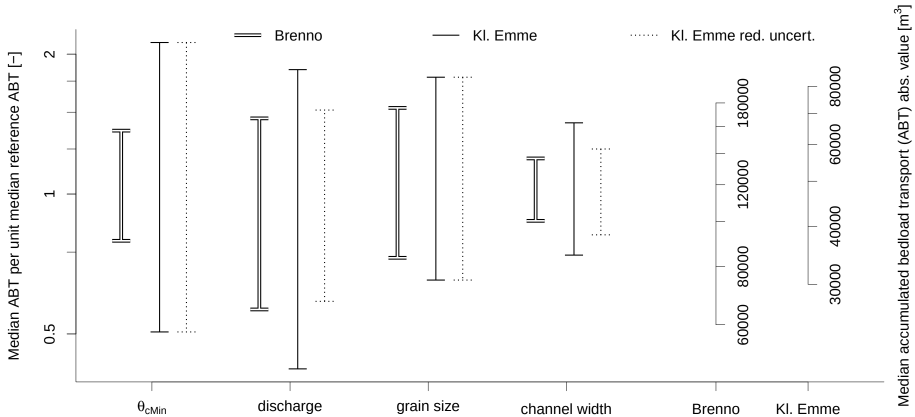

Figure 8. Simulation sensitivity with respect to simulated accumulated bedload transport (ABT) for different input parameters.

ESURFD
2, 773–822, 2014

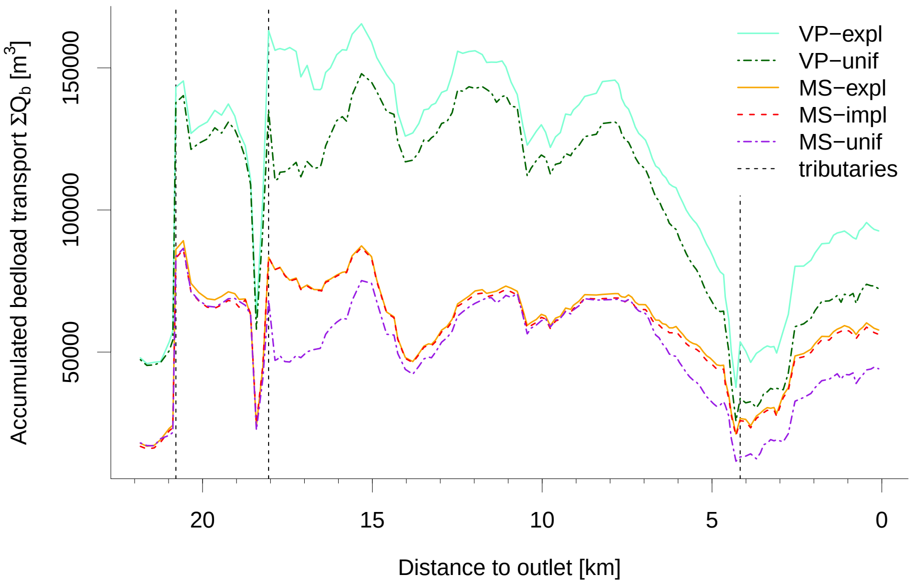

Figure 9. Comparison of simulated accumulated bedload transport in the Brenno for different combinations of flow routing schemes and flow resistance relations. Two flow resistance relations are shown: variable power relation given in Eq. (5) (denoted VP) and grain size dependent Manning–Strickler relation given in Eq. (6) (denoted MS). Three flow routing schemes are shown: explicit kinematic wave (denoted expl), implicit kinematic wave (denoted impl) and uniform discharge (denoted unif). The "VP-unif" curve (green dot-dashed line) is the same as the red line in the top panel of Fig. 7.

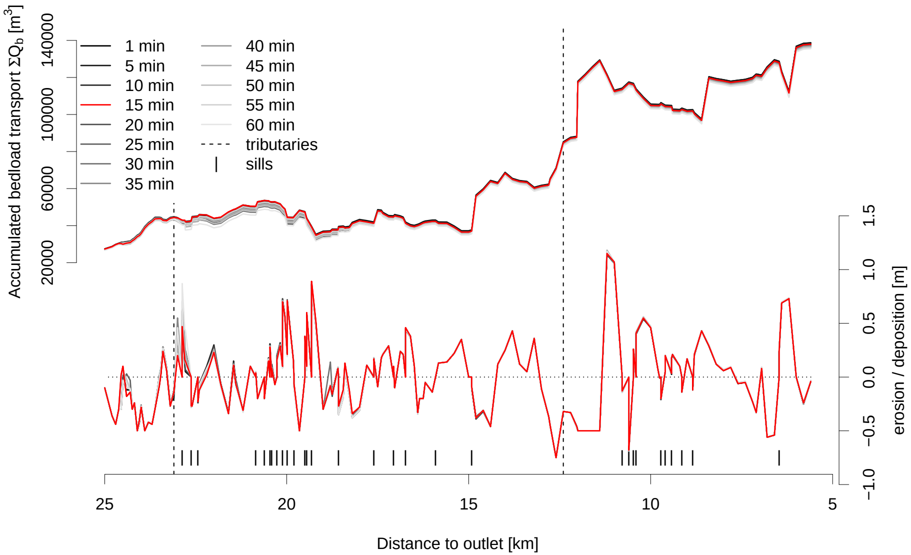

Figure 10. Comparison of simulated accumulated bedload transport and erosion and deposition in the Kleine Emme for different maximum time step lengths denoted in the plot legend. The maximum time step lenght value, which has been used for any other simulation in the Kleine Emme, is displayed in red.

ESURFD
2, 773–822, 2014

Recalculation of bedload transport observations

F. U. M. Heimann et al.

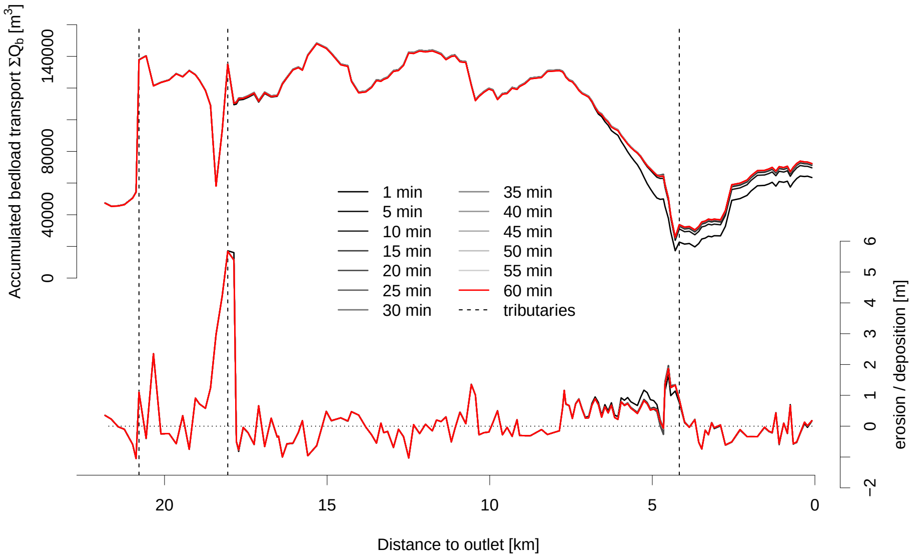

Figure 11. Comparison of simulated accumulated bedload transport and erosion and deposition in the Brenno for different maximum time step lengths denoted in the plot legend. The maximum time step lenght value, which has been used for any other simulation in the Brenno, is displayed in red.

ESURFD
2, 773–822, 2014

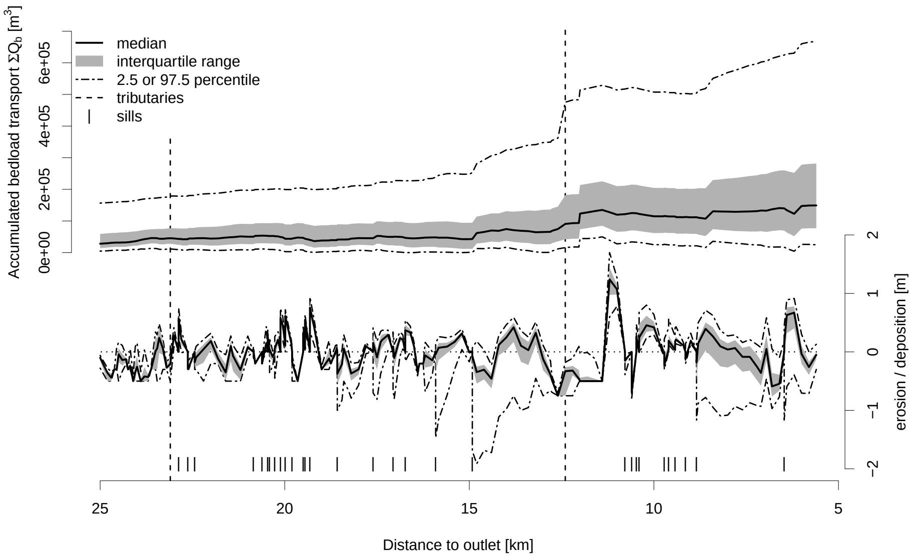

Figure 12. Output variability within sensitivity study for the Kleine Emme.

ESURFD
2, 773–822, 2014
Recalculation of bedload transport observations
F. U. M. Heimann et al.

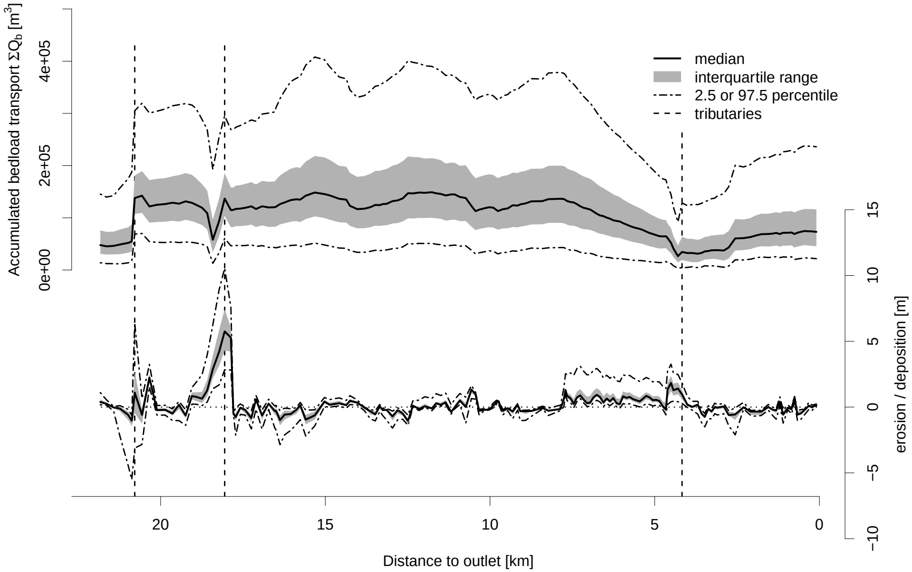

Figure 13. Output variability within sensitivity study for the Brenno.

ESURFD
2, 773–822, 2014

Recalculation of bedload transport observations

F. U. M. Heimann et al.

Figure 14. River bed of the Brenno at the confluence with the Riale Riascio exhibiting blocks with diameters of up to 2 m.

ESURFD

2, 773–822, 2014